American Mineralogist, Volume 81, pages 92–104, 1996

# Phonon spectra of alkali feldspars: Phase transitions and solid solutions

M. Zhang, B. Wruck, A. Graeme Barber, E.K.H. Salje, and M.A. Carpenter

Department of Earth Sciences, University of Cambridge, Downing Street, Cambridge CB2 3EQ, U.K.

## Abstract

The phonon spectra of IR-active vibrations in alkali feldspars have been systematically investigated in the spectral range 50–2000 $cm^{-1}$ at temperatures between 20 and 900 K. Samples with high degrees of Al-Si order display IR absorption line profiles with spectral line widths that are systematically smaller than those for samples with low degrees of Al-Si order. Phonon frequencies depend in a nonlinear manner on the Na-K content, indicating nonideal mixing properties. The mode Grüneisen parameters are largest for low-frequency lattice modes and Si-O stretching modes; some negative Grüneisen parameters were found at phonon energies below 430 $cm^{-1}$.

The temperature evolution of the phonon spectra shows clear indications of the $C2/m$-$C\bar{1}$ transition in Al-Si disordered Na-rich samples. An anomaly for highly Al-Si ordered microcline at 270 K is confirmed.

## Introduction

The structural state of feldspars need not be the same in every part of a crystal. In fact, local variations of the degree of Al-Si ordering and of the structural shear deformation associated with a structural phase transition are known to generate characteristic microstructures in feldspars (e.g., Brown and Parsons 1994; Smith and Brown 1988, for review). Mesoscopic microstructures with characteristic lengths of about 100 Å include tweed and stripe structures and incommensurate structures (Salje 1990, 1991, 1992a, 1992b, 1992c, 1993, 1994; Putnis and Salje 1994; Bratkovsky et al. 1994a, 1994b, 1994c; Tsatskis et al. 1994).

When such nonuniform samples are investigated one expects the results to depend sensitively on the characteristic length scale of the experiment. Measurements of volume quantities, such as the heat of solution and the specific heat, obviously integrate all structural effects. X-ray diffraction, on the other hand, leads to an average structure unless diffuse scattering is explicitly taken into account. The average structure often ignores the relevant microstructures and leads to some idealized approximation of the true structure. Transmission electron microscopy (TEM) reveals microstructures but usually fails to determine the local degree of Al-Si ordering and the local degree of Na-K exsolution. Other spectroscopic techniques focus on local structural parameters (Phillips et al. 1988; Petrov et al. 1993; Hofmeister and Rossman 1984). The interpretation of the spectra in terms of simple geometrical features is difficult for feldspars.

Probably the most sensitive tool for the determination of thermodynamic state parameters (e.g., degree of Al-Si order and the degree of exsolution) is phonon spectroscopy [e.g., hard-mode spectroscopy (Salje 1992c)]. Applications to feldspars were recently reviewed by Salje (1994); previous reviews of the experimental techniques and other applications include those of Bismayer (1990) and Salje (1992b). For feldspars it has been shown that: (1) The structural phase transition $C2/m$-$C\bar{1}$ in anorthoclase leads to an increase of the integral cross section of Raman signals at 473 and 514 $cm^{-1}$ (Salje 1986). (2) The local degree of Al-Si order can be determined by infrared spectroscopy in sodium feldspar using line shifts and intensity changes in the spectral region between 500 and 700 $cm^{-1}$ as indicators (Salje et al. 1989). (3) The effects of T1, T2, and T1o-T1m ordering can be separated in potassium feldspar (Harris et al. 1989). (4) Incommensurate potassium feldspars possess an intermediate degree of Al-Si ordering, which takes virtually no part in the structural modulation (Harris et al. 1989; Putnis and Salje 1994).

This paper reports the results of a new study of phonon effects in alkali feldspars, the goal of which is to characterize and quantify the structural effects of kinetic processes in feldspars and other minerals. Such kinetic processes were found to result in material that can be riddled with microstructures and defects. Laboratory experiments on sodium feldspar have shown that, despite these complications, systematic changes in phonon spectra occur during kinetic annealing and that these changes can be calibrated in terms of thermodynamic quantities (e.g., the degree of Al-Si ordering) (Salje and Kroll 1991; Wruck et al. 1991; Salje 1992a, 1992b, 1992c; Salje et al. 1993). We are now expanding this approach to alkali feldspars, including perthitic material. Prior to any such study of the kinetic processes, the phonon spectra must be calibrated. This was achieved by measuring the powder spectra of two solid-solution series of alkali feldspars: Al-Si ordered ($Q_{od} \approx 1$) and disordered ($Q_{od} \approx 0$) (Salje 1985;

0003–004X/96/0102–0092$05.00

**TABLE 1.** Lattice parameters of alkali feldspar samples used in this study

| Or (mol%) | a (Å) | b (Å) | c (Å) | α (°) | β (°) | γ (°) | V (Å³) |
|---|---|---|---|---|---|---|---|
| | | | **Al-Si ordered alkali feldspar series** | | | | |
| 98.8 | 8.588(2) | 12.966(2) | 7.224(2) | 90.62(2) | 115.96(1) | 87.71(2) | 722.7(3) |
| 90.1 | 8.552(2) | 12.962(2) | 7.219(2) | 90.66(2) | 115.93(1) | 87.65(2) | 719.1(4) |
| 81.8 | 8.520(2) | 12.960(2) | 7.215(2) | 90.80(2) | 115.93(1) | 87.60(2) | 715.8(4) |
| 75.1 | 8.483(2) | 12.955(2) | 7.218(2) | 90.90(3) | 115.91(2) | 87.60(2) | 712.9(4) |
| 65.2 | 8.441(3) | 12.947(2) | 7.211(2) | 91.17(2) | 115.92(2) | 87.58(2) | 708.2(5) |
| 55.4 | 8.398(2) | 12.934(2) | 7.204(1) | 91.47(2) | 115.97(1) | 87.53(1) | 702.8(3) |
| 50.8 | 8.367(4) | 12.926(3) | 7.208(4) | 91.75(3) | 115.98(2) | 87.49(3) | 700.0(7) |
| 35.6 | 8.296(4) | 12.887(3) | 7.193(3) | 92.68(3) | 116.16(3) | 87.58(2) | 689.3(7) |
| 20.1 | 8.219(3) | 12.842(3) | 7.178(2) | 93.51(3) | 116.39(2) | 87.69(2) | 677.3(4) |
| 11.3 | 8.181(2) | 12.811(2) | 7.168(2) | 94.97(2) | 116.44(2) | 87.61(2) | 671.0(3) |
| 0.4 | 8.137(2) | 12.784(2) | 7.159(2) | 94.30(2) | 116.60(1) | 87.71(1) | 664.1(3) |
| | | | **Al-Si disordered alkali feldspar series** | | | | |
| 98.8 | 8.601(2) | 13.024(2) | 7.180(2) | 90.0 | 116.01(1) | 90.0 | 722.9(3) |
| 78.0 | 8.513(1) | 13.022(1) | 7.173(1) | 90.0 | 115.99(1) | 90.0 | 714.7(2) |
| 69.1 | 8.477(1) | 13.013(1) | 7.170(1) | 90.0 | 116.02(1) | 90.0 | 710.8(3) |
| 62.5 | 8.445(1) | 13.010(1) | 7.169(1) | 90.0 | 116.05(1) | 90.0 | 707.7(2) |
| 54.8 | 8.407(2) | 13.013(2) | 7.163(2) | 90.0 | 116.10(2) | 90.0 | 703.8(4) |
| 46.9 | 8.374(2) | 12.994(2) | 7.158(2) | 90.0 | 116.10(2) | 90.0 | 699.4(4) |
| 37.6 | 8.324(3) | 12.980(4) | 7.154(3) | 90.41(4) | 116.14(2) | 90.08(3) | 693.8(6) |
| 29.4 | 8.284(3) | 12.965(3) | 7.152(3) | 91.49(3) | 116.28(2) | 90.09(2) | 688.4(6) |
| 17.6 | 8.236(1) | 12.929(2) | 7.135(1) | 92.45(2) | 116.37(1) | 90.11(1) | 679.9(3) |
| 8.8 | 8.195(2) | 12.892(2) | 7.125(2) | 93.10(2) | 116.37(1) | 90.11(1) | 673.2(3) |
| 0.4 | 8.152(1) | 12.867(2) | 7.110(1) | 93.52(2) | 116.44(1) | 90.19(1) | 666.2(3) |

*Note:* Standard errors are given in parentheses and refer to the last decimal places.

Salje et al. 1985). The temperature dependence of phonon spectra were analyzed for the following compositions: $Ab_{100}$, $Or_{100}$, $Ab_{25}Or_{75}$, and $Ab_{45}Or_{55}$ with approximately complete Al-Si order, and $Ab_{71}Or_{29}$, $Ab_{62}Or_{38}$, and $Or_{100}$ with complete long-range Al-Si disorder.

The paper is organized as follows. First, the experimental procedure is described, then the spectra are given, and, finally, the analysis is summarized. The relevant equations and their justifications were published previously by Salje (1992b, 1994). In a forthcoming paper we will show that natural samples of alkali feldspar can be analyzed using the spectra given in this paper as a basic set for comparison (i.e., the primary spectra). For the quantitative analysis we normalize all primary spectra and combine all possible pairs of primary spectra into a new set of secondary spectra. These secondary spectra correspond to mechanical mixtures of the pairs of primary compounds (i.e., those described in this paper). Such mixtures can, for example, correspond to lamellae in alkali feldspars in which the lamellae have different chemical compositions and different degrees of Al-Si order. Spectra of natural samples are then compared with such secondary spectra, and the closest match between the spectrum of an unknown sample and any secondary spectrum is determined numerically. It is the purpose of this paper to describe how the primary spectra were obtained and to discuss some of their most obvious spectroscopic features.

## EXPERIMENTAL METHODS

### Sample preparation

Two solid-solution series of ordered and disordered alkali feldspars were produced by ion exchange according to the method of Kroll et al. (1980).

For the ordered solid solution, starting material was a pure and well-ordered albite from Alp Rischuna, Valais, Switzerland (Harker Collection no. 5028, Department of Earth Sciences, Cambridge). Its chemical composition as determined by electron microprobe is Ab 99.6 mol%, Or 0.4 mol%. A K end-member was produced by ion exchange of this albite in molten KCl (weight ratio 1:60) at 1125 K for 6 h. The electron microprobe analysis gave Ab 1.2 mol%, Or 98.8 mol%. Proportions of these two end-members were then thoroughly mixed, pressed into pellets, wrapped in platinum foil, and homogenized at 1175 K for 3 d.

To produce the disordered series, the starting albite was first converted into analbite. Dry annealing at 1365 K for 28 d was not sufficient, as checked by X-ray powder diffraction, and the sample was therefore annealed hydrothermally ($P_{H_2O}$ = 200 bar) at 1255 K for 8 d. The disordered solid-solution series was then prepared in a manner analogous to that used for the ordered series, as described above, except that the samples were homogenized at 1275 K. The chemical compositions of the end-products were determined by comparison of their lattice parameters with those published by Kroll et al. (1986).

The lattice parameters of all samples were determined by X-ray Guinier powder diffraction and are given in Table 1. For each sample, between 41 and 50 diffraction lines were measured and used to fit the lattice parameters using a standard least-square refinement procedure. The standard deviations are also listed in Table 1. The Al-Si ordered samples have a degree of order greater than 90%; they are denoted as $Q_{od} \approx 1$. Al-Si disordered samples show the displacive phase transition without any visible defect tail, which indicates that the samples are fully dis-

**TABLE 2.** Experimental details for the various infrared absorption experiments

| Matrix | PW (mg) | AS (mg) | IR region ($cm^{-1}$) | Source | Detector | Beamsplitter | T region (K) | Window |
|---|---|---|---|---|---|---|---|---|
| Polyethylene | 100 | 2.00 | 50–500 | Hg-Arc | DTGS | Mylar 6 μm | 20–315 | polyethylene |
| Polyethylene | 100 | 2.00 | 50–500 | Hg-Arc | DTGS | Mylar 6 μm | 293–350 | none |
| Silicon wafer | | ~2.40 | 50–450 | Hg-Arc | DTGS | Mylar 6 μm | 300–550 | none |
| CsI | 300 | 0.87 | 250–700 | Globar | DTGS | Mylar 3.5 μm | 20–750 | KRS-5 |
| CsI | 300 | 0.67 | 450–2000 | Globar | MCT | KBr | 60, 294 | KRS-5 |
| KBr | 200 | 0.50 | 450–2000 | Globar | MCT | KBr | 20–900 | KRS-5 |

*Note:* PW = pellet weight, AS = amount of sample, T region = temperature region, Window = the windows used with the cryostat for low-temperature experiments, DTGS = room temperature FIR DTGS detector, MCT = liquid nitrogen–cooled MCT detector; the silicon wafer was 0.5 mm thick with one side polished.

ordered ($Q_{od} = 0$). No attempt was made to determine the value of $Q_t$ numerically.

### Infrared absorption spectra

Samples were crushed and milled in an agate mortar in a Spex microball mill for 35 min. The even-sized fine-grained powder was kept in a drying oven at 395 K to ensure that no water contamination occurred prior to the preparation of the IR pellets. Three types of pellets were used for the different frequency ranges (Table 2). For the far IR region, samples were heated (from 300 to 550 K) by using powdered sample rubbed onto a silicon wafer or by using powder pressed between two silicon wafers.

The spectra were recorded under vacuum at temperatures between 20 and 900 K using a Bruker 113V FT-IR instrument. For sample heating, the specimen was positioned within a cylindrical platinum-wound furnace. The temperature was measured using a Pt/PtRh thermocouple, which was pressed against the sample. The temperature stability was less than ±1 K and a heating rate of 8–15 K/min was used. During the heating sequences, samples were held at each temperature for at least 15 min to allow thermal equilibration before commencing the IR data collection. Low-temperature spectra were measured with the pellet mounted inside a closed-cycle Leybold cryostat. A copper mesh was in direct contact with the pellet to ensure good thermal contact between the sample and the cold finger. Spectra were recorded in both cooling and heating sequences. The temperature stability was ±0.5 K. The spectra were collected using a liquid nitrogen–cooled MCT detector for MIR and a room temperature DTGS detector for FIR. The spectral resolution function of the 113V instrument was set to 1 or 2 $cm^{-1}$ for MIR and 2 or 4 $cm^{-1}$ for FIR. This function sets a lower limit for the measured line width but has practically no effect on the determination of the spectral position of the phonon signal. It does not limit the resolution for the determination of relative changes in the line width if proper deconvolution of the line profiles is carried out. The procedure for the determination of the absorption spectra was as follows: Each spectrum was calculated by Fourier transformation of 512 interferometer scans. All spectra

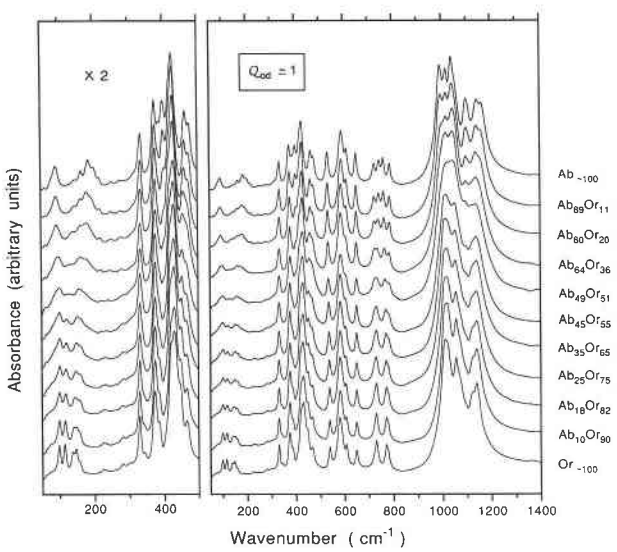


**FIGURE 1.** Infrared absorption spectra of Al-Si ordered alkali feldspars measured at room temperature (294 K). The range 50–500 $cm^{-1}$ is repeated at a larger scale on the left side to show detailed variations more clearly. The content of potassium feldspar is shown as the Or component in mole percent.

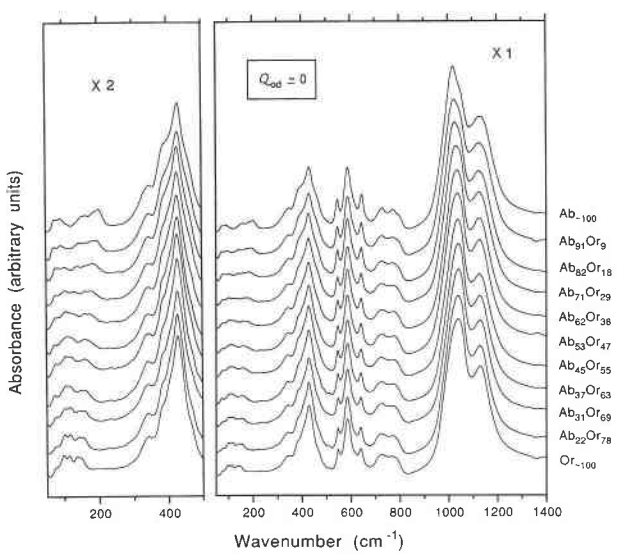


**FIGURE 2.** Infrared absorption spectra of Al-Si disordered alkali feldspars measured at room temperature. The range 50–500 $cm^{-1}$ is shown at a larger scale on the left side, as in Figure 1.

**TABLE 3.** Mode Grüneisen parameters at 300 K and tentative mode assignments (Iiishi et al. 1971a, 1971b)

| Albite ($Ab_{100}$, $Q_{od}$ = 1) | | | Microcline ($Or_{100}$, $Q_{od}$ = 1) | | |
|---|---|---|---|---|---|
| $\omega_i$ ($cm^{-1}$) | $\gamma_i$ | Description | $\omega_i$ ($cm^{-1}$) | $\gamma_i$ | Description |
| 90 | | Na-O stretching | 96 | −0.91 | K-O stretching |
| 145 | | Na-O stretching | 113 | 4.27 | K-O stretching |
| 164 | 2.67 | Na-O stretching | 137 | 3.06 | K-O stretching |
| 185 | 4.35 | Na-O stretching | 146 | 3.96 | K-O stretching |
| 201 | 3.90 | Na-O stretching | 157 | 0.86 | K-O stretching |
| 216 | −0.74 | Na-O stretching | 223 | | |
| 251 | | Si-O-Al deformation or torsion | 232 | | Si-O-Al deformation or torsion |
| 276 | | Si-O-Al deformation or torsion | 280 | | Si-O-Al deformation or torsion |
| 318 | | | 302 | | |
| 334 | −0.14 | Si-O-Si(Al) deformation and torsion | 329 | 0.43 | Si-O-Si(Al) deformation and torsion |
| 374 | | | 344 | −0.92 | Si-O-Si(Al) deformation and torsion |
| 387 | 0.24 | Si-O-Si(Al) deformation and torsion | 373 | | |
| 400 | −1.07 | Si-O-Si deformation | 386 | 1.16 | |
| 416 | 0.30 | Si-O-Si deformation | 405 | | Si-O-Si deformation |
| 429 | −0.33 | | 418 | −0.30 | |
| 462 | 1.10 | | 432 | | |
| 476 | 0.82 | Coupling between O-Si-O deformation and Na-O stretching | 446 | 1.82 | Si-O-Si deformation |
| 497 | | | 467 | 0.34 | Coupling between O-Si-O bending and K-O stretching |
| 531 | 0.43 | | 537 | 0.45 | |
| 589 | 0.58 | O-Si(Al)-O bending | 580 | 0.40 | O-Si(Al)-O bending |
| 611 | 0.59 | O-Si(Al)-O bending | 607 | 0.48 | O-Si(Al)-O bending |
| 650 | 0.32 | O-Si(Al)-O bending | 648 | 0.51 | O-Si(Al)-O bending |
| 732 | 0.42 | Si-Al(Si) stretching | 716 | | Si-Al(Si) stretching |
| 744 | 1.25 | Si-Al(Si) stretching | 728 | 1.74 | Si-Al(Si) stretching |
| 761 | 0.54 | Si-Si stretching | 769 | 0.51 | Si-Si stretching |
| 781 | 0.92 | Si-Si stretching | 778 | 0.09 | Si-Si stretching |
| 994 | 0.70 | Si(Al)-O stretching | 1007 | 0.75 | Si(Al)-O stretching |
| 1018 | 0.72 | Si(Al)-O stretching | 1017 | 1.14 | Si(Al)-O stretching |
| 1040 | 0.65 | Si(Al)-O stretching | 1054 | 1.02 | Si(Al)-O stretching |
| 1058 | 0.29 | | 1073 | 1.02 | |
| 1102 | 1.35 | Si-O stretching | 1091 | | Si-O stretching |
| 1142 | 1.32 | Si-O stretching | 1118 | 0.99 | Si-O stretching |
| 1162 | 1.74 | Si-O stretching | 1138 | 1.13 | Si-O stretching |

were then recorded as absorbance $\alpha$, with $\alpha = -\log_{10}(I_{sample}/I_{reference})$, where $I$ is the single-beam transmission intensity. Profile analysis of the spectra was achieved by fitting of Lorentzian peak profiles to the recorded absorption spectra using the program RAZOR (Spectrum Square Assoc., Inc.). The errors for the determination of peak positions and widths are on the order of 0.2 $cm^{-1}$. The absolute integrated absorbance of a phonon signal was reproducible between different samples to within 5%.

## RESULTS

The infrared powder-absorption spectra, recorded at room temperature, in the region 50–1400 $cm^{-1}$ for the fully ordered and disordered alkali feldspar solid-solution series are shown in Figures 1 and 2, respectively. It is clearly seen that the fully ordered series ($Q_{od} \approx 1$) shows phonon signals with small line widths and every spectral feature well resolved, whereas the disordered series ($Q_{od} = 0$) exhibits broad peaks resulting from random Al-Si distributions. The variation of composition causes frequency shifts and changes in band intensities. Iiishi et al. (1971a, 1971b) assigned the absorption bands as shown in Table 3. A spurious absorption band of polyethylene at 74 $cm^{-1}$ is seen in some spectra. The infrared spectra recorded at various temperatures for fully Al-Si ordered $Ab_{100}$, $Or_{100}$, and $Or_{55}Ab_{45}$ are shown in Figures 3–5. Two examples of Al-Si disordered samples, $Or_{38}$ and $Or_{29}$ (Figs. 6 and 7, respectively), were selected because the crystals undergo structural phase transitions. The spectral features related to the phase transitions will be discussed in a later section.

The temperature dependence of a vibrational mode frequency arises mainly from two contributions: (1) a volume contribution owing to thermal expansion and (2) a pure temperature (volume-independent) contribution originating from anharmonic interatomic interactions, phonon scattering, and atomic shifts that do not directly contribute to thermal expansion. We first describe the most characteristic temperature effects on the phonon.

The effect of increasing temperature on the phonon spectra is quite clearly seen in the spectra shown in Figures 3–7 as an increase in band widths and also a shift in frequencies. Several phonon bands can easily be resolved at low temperatures but not at room temperature. For example, the bands at 768 and 726 $cm^{-1}$ ($Or_{100}$, $Q_{od} \approx 1$) are spectral shoulders at room temperature but are resolved as separate peaks at 20 K. Similarly, a phonon signal at 497 $cm^{-1}$ ($Ab_{100}$), which was predicted by von Stengel (1977), is clearly resolved at 40 K in our spectra. Further phonon signals, at 318 and 416 $cm^{-1}$ ($Ab_{100}$, $Q_{od} \approx 1$) and at 281 and 406 $cm^{-1}$ ($Or_{100}$, $Q_{od} \approx 1$), were observed for the first time. To illustrate the effect of temperature, the phonon spectra of $Ab_{100}$ ($Q_{od} \approx 1$) for $T$ = 23 and 600 K are shown in Figure 8. It is seen in this figure that all phonon signals display much reduced line

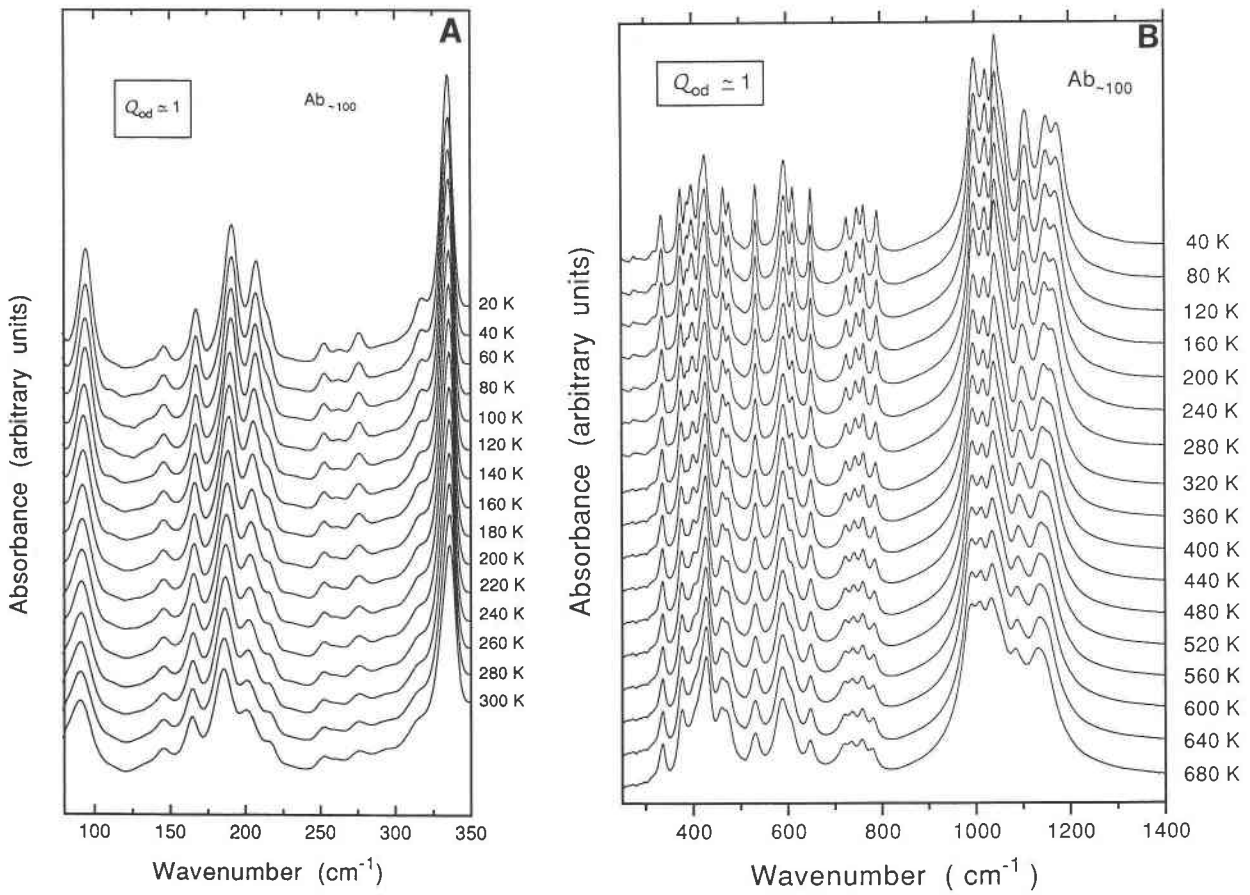


**FIGURE 3.** Temperature evolution of infrared absorption spectra of Al-Si ordered sodium feldspar ($Ab_{100}$, $Q_{od} \simeq 1$). **(A)** Low-temperature spectra, 70–350 $cm^{-1}$. **(B)** Low- and high-temperature spectra at 250–1400 $cm^{-1}$.

widths at low temperatures and shifts of their phonon frequencies. The thermal frequency shifts are large both for Si-O stretching modes and for low-frequency modes that may involve the movements of Na or K.

For $Or_{100}$ ($Q_{od} \approx 1$), an intensity anomaly is observed. As shown in Figure 4, the peak profiles in the region 96–158 $cm^{-1}$ change unusually strongly with temperature. The mode at 157 $cm^{-1}$ (value at room temperature) becomes more intense at low temperature. This mode is assigned as K-O stretching motion and T-O-T bending (von Stengel 1977). We will argue later that this mode is associated with a structural instability in microcline ($Or_{100}$, $Q_{od} \approx 1$).

It is also evident that the bands for ordered feldspar ($Q_{od} \approx 1$) are much broader than the bands for other framework structures where line widths are below 4 $cm^{-1}$ at 30 K (Salje 1992c). Line broadening is particularly strong for Si-O stretching modes between 1000 and 1200 $cm^{-1}$. This observation is not an artifact of the spectrometer, as seen from a comparison with spectra of other materials that do, indeed, show much reduced line width, even for highly absorbing stretching modes. Similar broad stretching modes in feldspars were reported in previous publications (Laves and Hafner 1956; Iiishi et al. 1971a; von Stengel 1977; Salje et al. 1989; Harris et al. 1989).

## ANALYSIS OF THE SPECTRA

### The effect of chemical mixing

The spectra of the end-member sodium and potassium feldspars are identical, within the experimental resolution discussed before, to those published by Harris et al. (1989) and Salje et al. (1989). The solid-solution series for $Q_{od} = 0$ and $Q_{od} \approx 1$ show continuous changes in the spectra with changing composition. The spectral changes can be described in two ways depending on their spectral range. Phonons with frequencies higher than ca. 300 $cm^{-1}$ show an almost linear change in phonon frequency with changing chemical composition. These phonons are, thus, related mainly to the tetrahedral network and do not correlate with individual Na-O or K-O bonds. The effect of Na-K mixing on these high-frequency phonons is due to a global distortion of the entire crystal structure with the corresponding change in tetrahedral bond angles and distances.

This behavior can be contrasted with that of low-fre-

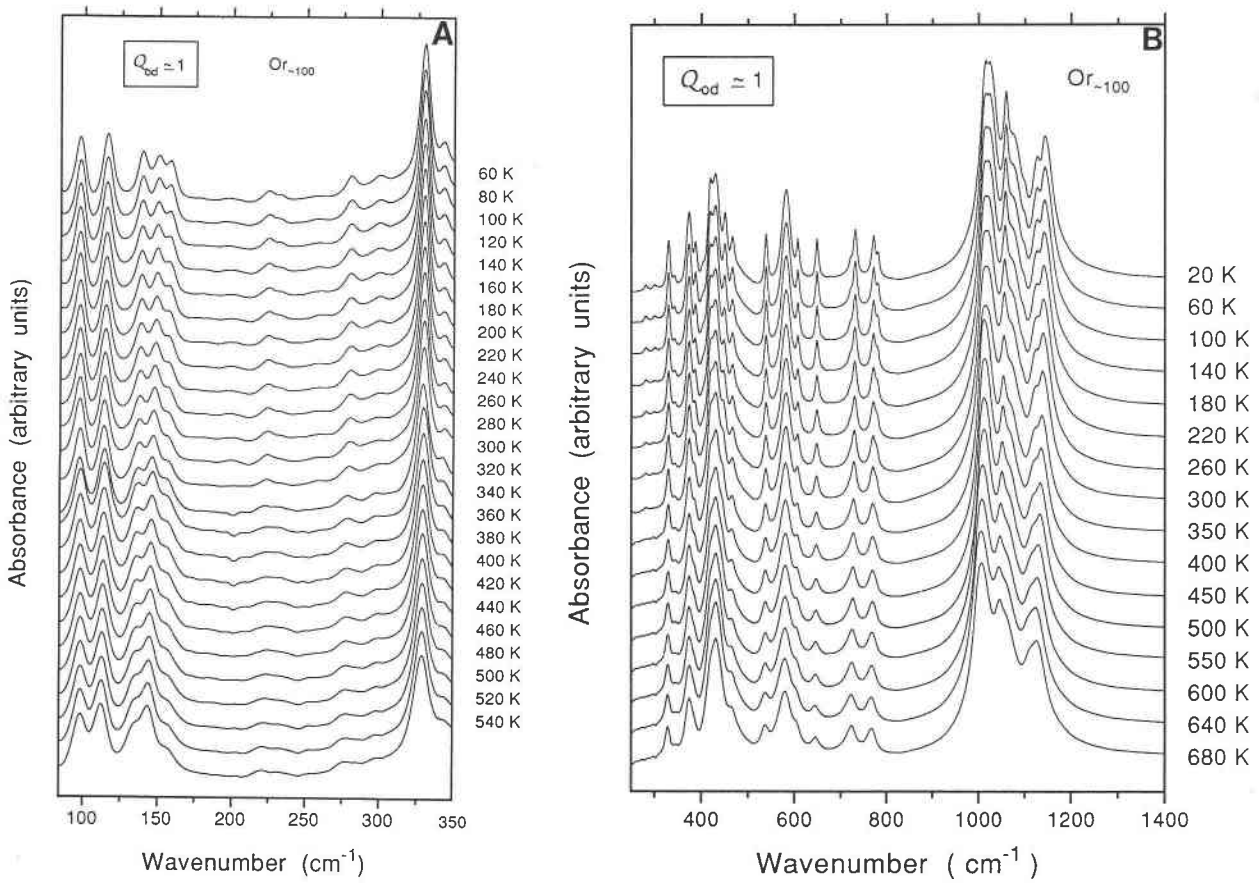


**FIGURE 4.** Temperature evolution of infrared absorption spectra of microcline ($Or_{100}$, $Q_{od} \simeq 1$). Low- and high-temperature spectra in the spectral range 80–350 $cm^{-1}$ **(A)** and 250–1400 $cm^{-1}$ **(B)**.

quency phonons. These phonons relate mainly to vibrations between the large cations and the surrounding structure. This effect is best seen for the $Q_{od} \approx 1$ series because the phonon signals are not broadened by the additional Al-Si disorder. Comparing the spectra of $Ab_{45}Or_{55}$ with those of the sodium and potassium feldspars, one observes that the spectrum of a binary feldspar is not simply the superposition of the spectra of the end-members but contains additional phonon signals (Fig. 9). In Figure 9, the samples $Or_{100}$ and $Ab_{100}$ display peak profiles with similar line widths. It is not possible to fit the spectrum of $Ab_{45}Or_{55}$ with the same profiles and the same number of phonon signals, however. Numerical analysis shows that all phonons of the end-members appear as rather weak signals in the mixed crystals, although with slightly shifted peak positions. In addition to these signals, further phonon signals with generally larger intensities are found. A full analytical analysis appears impossible, however, because refinements of the spectral functions do not converge to a unique solution. It may be possible to separate the various phonon signals using spectra from single crystals rather than powder. In the context of this paper it suffices to note that the mixing properties of alkali feldspars are not ideal and that the phonon signals at low frequencies are not simply determined by the cage structure around the alkali atoms but involve the interaction with atomic positions beyond the nearest neighbors.

A further indication of nonideal mixing stems from the observation that phonon lines at higher frequencies are not shifted linearly with respect to the end-members. In Figure 10 some relative changes in the absorption spectra with composition are shown. Note that several of the connecting lines for the phonon frequencies are not straight lines; they are systematically bent. Within the box drawn on Figure 10, only a few of the most prominent signals are given. The fact that both the shifts of the high-frequency modes and the mixing of the low-frequency modes are not linear functions of chemical composition indicates that the phononic excess enthalpy $\Delta H$ and entropy $\Delta S$ are also nonlinear functions of the Na:K ratio. The excess quantities $\Delta H$ and $\Delta S$ could, in fact, be calculated from the relative shift of the phonon frequencies $\Delta\omega$ if the full dispersion relationships were known. The nonideal mixing properties of the alkali feldspar correspond directly to these phonon renormalizations, although further contributions may possibly arise. The observed pho-

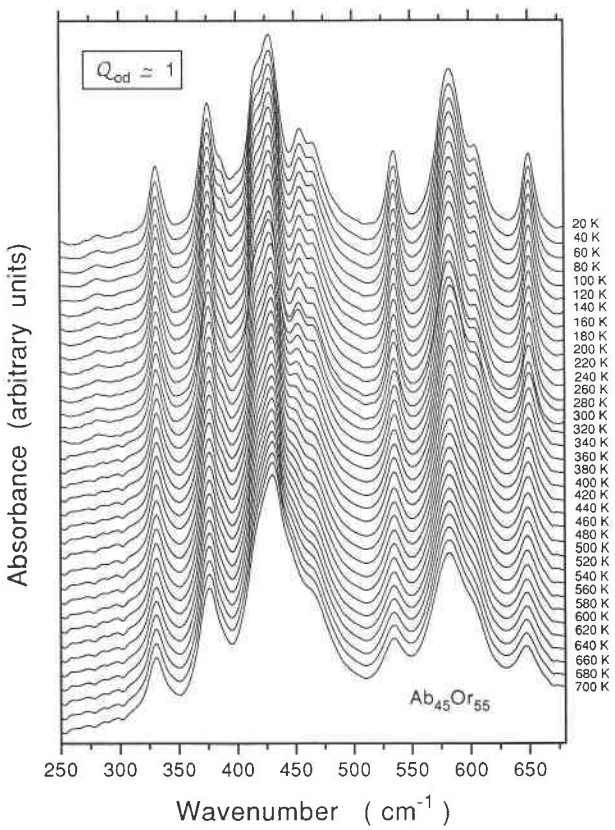


**FIGURE 5.** Infrared spectra of $Ab_{45}Or_{55}$ ($Q_{od} \simeq 1$) at low and high temperatures (250–680 $cm^{-1}$).

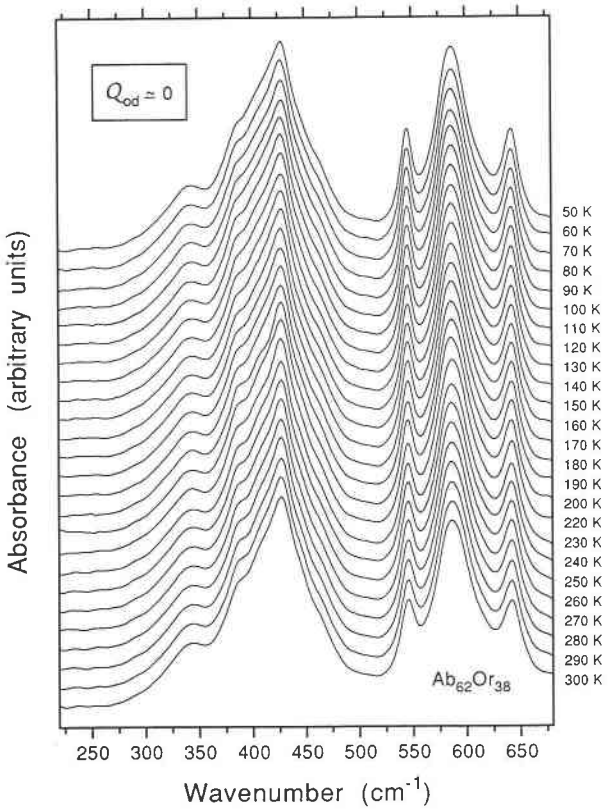


**FIGURE 6.** Temperature dependence of the phonon spectra of $Ab_{62}Or_{38}$ ($Q_{od} = 0$) at low temperatures in the spectral range 220–680 $cm^{-1}$.

non behavior is consistent with the nonideal behavior found in calorimetric measurements by Haselton et al. (1983).

### The temperature dependence of phonon signals from samples with $Q_{od} = 0$

The temperature evolution of the phonon spectra of $Or_{100}$ ($Q_{od} = 0$, sanidine) shows no significant anomalies. The most clearly observed phonon shifts are seen in the mid-IR region (Fig. 11). Comparing these shifts with the thermal volume ($V$) expansion at room temperature (Henderson 1979) leads to mode Grüneisen parameters $\gamma_i$, $\gamma_i = -[d(\ln \omega_i)/d(\ln V)]$, with $\gamma_{535\ cm^{-1}} = 0.43$.

A more significant change in the phonon spectra was found for binary feldspars with large proportions of Ab component. The temperature evolution of the phonon frequency near 544 $cm^{-1}$ ($Ab_{62}Or_{38}$, $Q_{od} = 0$) in Figure 12 shows a change in slope at the temperature of the displacive phase transition $C2/m$-$C\bar{1}$. The transition temperature is 235 K. With $\Delta(\omega^2) \propto Q^2 \propto |T - T_c|^{2\beta}$, we find $\beta = 1/2$, i.e., the phase transition follows classical second-order Landau-type behavior. This transition is also seen in $Ab_{71}Or_{29}$ ($Q_{od} = 0$) (Fig. 13) as a change in line width with decreasing temperature. The transition temperature is 465 K. The same phase transition was previously observed for $Ab_{71}Or_{29}$ ($Q_{od} = 0$) using Raman spectroscopic techniques (Salje 1986) and for lower proportions of Or component by X-ray powder diffraction (Harrison and Salje 1994). The phase diagram of the $C2/m$-$C\bar{1}$ transition ($Q_{od} = 0$) is shown in Figure 14. The transition temperature as a function of composition exhibits a linear behavior for intermediate compositions and a value reduced with respect to the extrapolation to the Na–end-member composition (Salje et al. 1991a).

The phase transition is also seen at room temperature when spectra with different Or contents are compared (Fig. 15). The transition composition is determined by the change in slope of the phonon frequencies near 640 and 1030 $cm^{-1}$. Interpolation of the data in Figure 15 leads to a chemical composition for the transition at room temperature near $Or_{37}Ab_{63}$, which is virtually identical to the value $Or_{36}Ab_{64}$ determined by Kroll et al. (1986).

The order parameter $Q$ of the phase transition $C2/m$-$C\bar{1}$ ($Q_{od} = 0$) is defined as unity for $Ab_{100}$ at $T = 0$ K and decreases with increasing Or content [ignoring all effects of quantum saturation (Salje et al. 1991b, 1991c)]. The transition finally disappears at $T = 0$ K for Or contents of $\gtrsim 50\%$. Theoretical analysis (Salje 1985, 1992a) predicts that the specific-heat anomaly near $T_c$ becomes smaller with increasing Or component (i.e., decreasing $T_c$). Simultaneously all other thermodynamic excess parameters related to the structural phase transition also

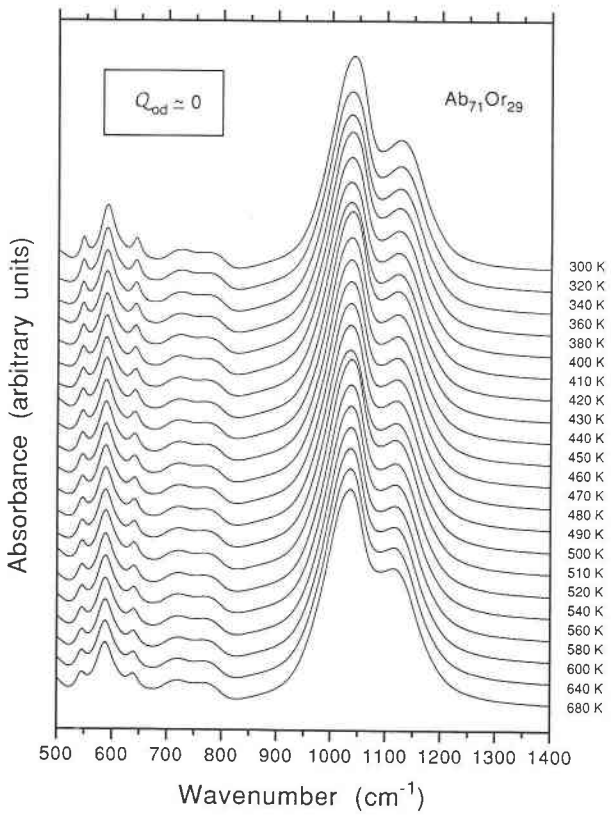


FIGURE 7. Phonon spectra of $Ab_{71}Or_{29}$ ($Q_{od} = 0$) at high temperatures (490–1400 cm$^{-1}$).

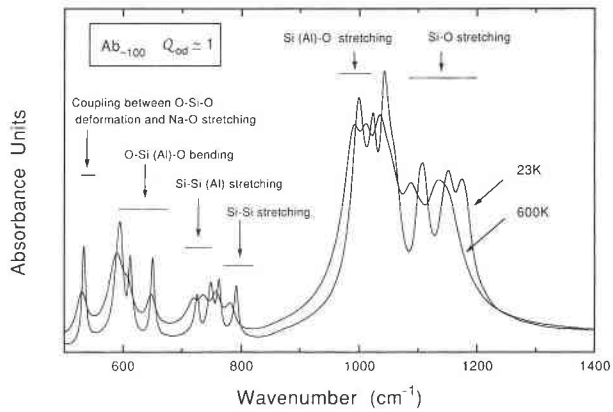


FIGURE 8. Comparison of phonon spectra at 23 and 600 K for Al-Si ordered sodium feldspar.

decrease with decreasing $T_c$. This trend explains why the anomaly is rather weak for $Or_{38}$ compared with the larger anomalies that occur at $Or_{29}$. Even larger anomalies are expected for samples with lower Or content.

### Temperature evolution of phonon signals from samples with $Q_{od} \approx 1$

The absorption spectra of $Ab_{100}$, $Ab_{25}Or_{75}$, and $Or_{100}$ (all $Q_{od} \approx 1$) show a softening of most phonons with increasing temperature. Such modes possess positive mode Grüneisen parameters. Phonon hardening, i.e., negative mode Grüneisen parameters, were observed for modes at 216, 334, 391, and 429 cm$^{-1}$ in $Ab_{100}$ and 96, 344, 406, and 418 cm$^{-1}$ in $Or_{100}$. In Figure 16 the temperature evolution of the 534 and 606 cm$^{-1}$ modes of the four compounds are shown. The softening is ca. 1 cm$^{-1}$ for 400 K. Plotting the data for the end-member compositions as a function of the unit cell volume (Fig. 17) shows the linear dependencies, with mode Grüneisen parameters between 0.3 and 0.55. The numerical values for several mode Grüneisen parameters are listed in Table 3. The typical error for the determination of these Grüneisen parameters is 0.05.

Inspection of Table 3 reveals two systematic trends. First, the mode Grüneisen parameters show the largest values (both positive and negative) for low-frequency modes involving the movement of Na, K, or both. This observation is understandable in terms of the relatively weak bonds between the alkali atoms and the tetrahedral network. Compression of the crystal has the largest effect around the alkali atoms and modifies the relevant phonon frequencies. In this sense, we can depict the cages around the alkali atoms as the softest configuration in the feldspar structure.

The second trend shows a surprising softness of the $SiO_4$ and $AlO_4$ tetrahedra. Tetrahedral stretching modes show mode Grüneisen parameters of the order of unity. These Grüneisen parameters are defined with respect to the volume change in the total crystal structure, and we may well envisage that this volume change is related more

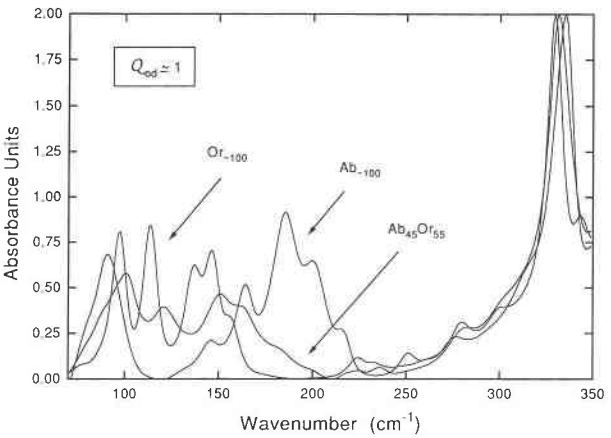


FIGURE 9. Comparison of the low-frequency part of the infrared absorption spectra of albite ($Ab_{100}$, $Q_{od} \simeq 1$), microcline ($Or_{100}$, $Q_{od} \simeq 1$), and an intermediate composition ($Ab_{45}Or_{55}$, $Q_{od} \simeq 1$). The phonon signal near 330 cm$^{-1}$ shows a gradual shift of the phonon frequency with chemical composition. In contrast to this behavior, the signals below 300 cm$^{-1}$ are composed of several phonon bands that are not related by simple frequency shifts. The spectra of the intermediate compounds are not a simple superposition or linear interpolation of the phonon signals of the two end-members, indicating nonideal mixing properties.

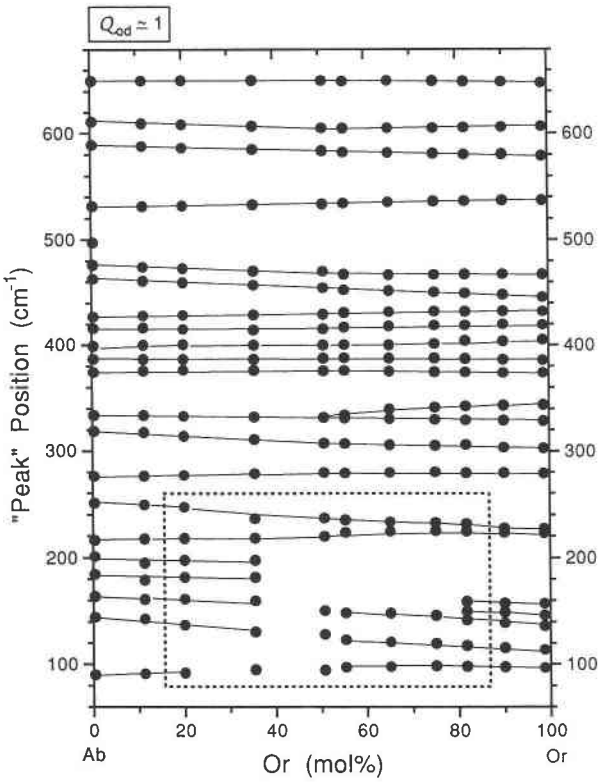


FIGURE 10. The maxima of Lorentzian peaks fitted to the absorption spectra as a function of chemical composition. Such peak maxima are easily distinguished at frequencies above ca. 300 cm$^{-1}$ and represent phonon signals. At lower frequencies they represent an empirical quantification of the spectra with additional phonon signals not represented in this graph (see Fig. 9 for comparison). Within the boxed area, only the strongest signals are shown.

to changes in Si-O-Si angles than to changes in tetrahedral size (Downs et al. 1992). If the Grüneisen parameters of the stretching modes were defined with respect to the tetrahedral volume itself, the values would be even greater than those in Table 3.

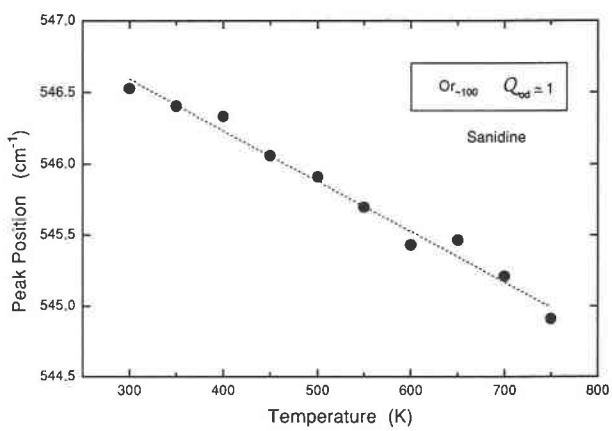


FIGURE 11. Temperature dependence of the 535 cm$^{-1}$ phonon in sanidine ($Or_{100}$, $Q_{od} \simeq 1$).

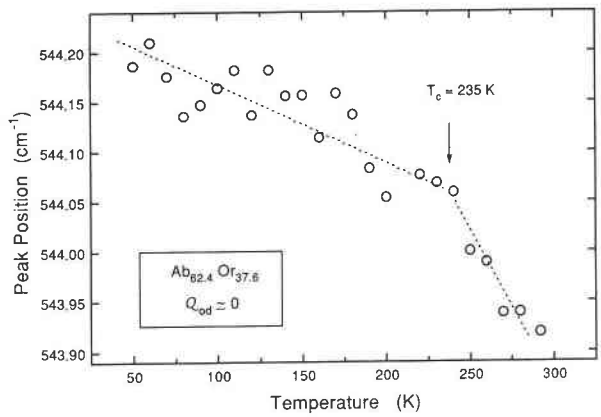


FIGURE 12. Thermal frequency shift of the 544 cm$^{-1}$ phonon with a structural phase transition $C2/m$-$C\bar{1}$ at $T_c$ = 235 K ($Ab_{62.4}Or_{37.6}$, $Q_{od}$ = 0).

The large values of the Grüneisen parameters for the Si-O stretching modes contrast with the smaller values for the bending modes. In terms of the deformation of the $SiO_4$ tetrahedra, we expect that the Si-O distances increase with increasing temperature, whereas the shape of the tetrahedra (e.g., the O-Si-O angles) remains rather unchanged. This appears to be a counterintuitive result for a highly anisotropic structure such as feldspar. It is also markedly different from the behavior in quartz (Barron et al. 1982). The mode Grüneisen parameters of the stretching modes of $\alpha$-quartz are below 0.07, or even negative, whereas the bending modes have Grüneisen parameters typically between 0.4 and 1. Such values correspond to a deformation of the shape of the $SiO_4$ tetrahedra and changes in their tilts, but there is little change in the Si-O distances. The behavior of feldspar appears to be very different indeed; Grüneisen parameters of the stretching modes are more than one order of magnitude larger than in $\alpha$-quartz, whereas those of the

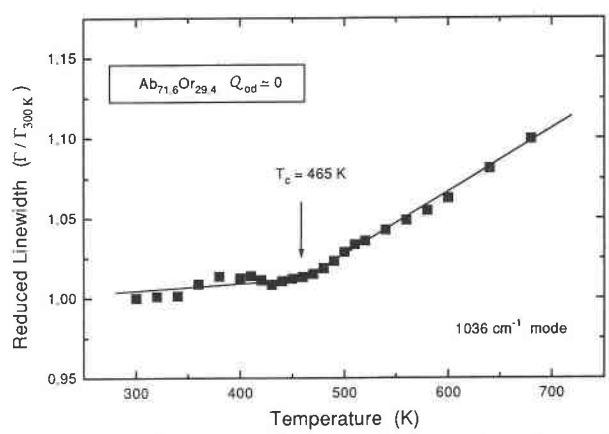


FIGURE 13. The change in the temperature dependence of the reduced line width of the 1036 cm$^{-1}$ mode in $Ab_{71.6}Or_{29.4}$ ($Q_{od}$ = 0) at 465 K corresponds to the structural phase transition $C2/m$-$C\bar{1}$.

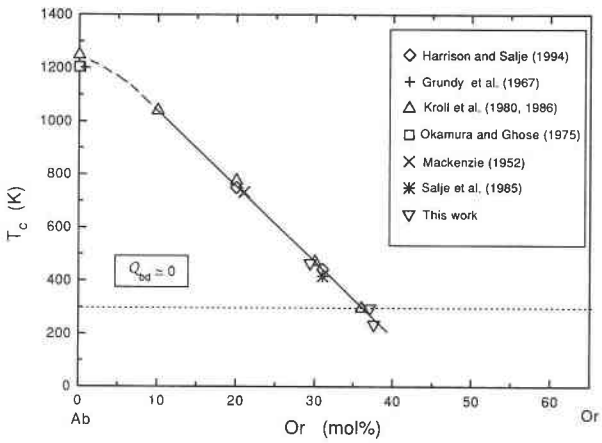


**FIGURE 14.** Compositional dependence of the phase transition temperature $T_c$ ($C2/m$-$C\bar{1}$). The phase transition remains second order for all compositions.

bending modes are slightly reduced. This observation certainly merits further attention from geometrical, structure analytical, and spectroscopic perspectives.

We now turn to the discussion of the temperature dependence of the phonon widths Γ. Data for the phonons at 761 and 533 $cm^{-1}$ ($Ab_{100}$, $Q_{od} \approx 1$) are shown in Figure 18, for example. They follow a temperature dependence of the type $\Gamma = A + BT + CT^2$ at $T > 300$ K, as described previously by Salje (1986). A linear correlation is found between the phonon frequencies and thermal line broadening for the phonon signal near 532 $cm^{-1}$ at four compositions (Fig. 19). A frequency softening of 1 $cm^{-1}$ is equivalent to line broadening of about 4 $cm^{-1}$. The linear relationship between $\Delta\omega$ and Γ was previously observed for changes in the degree of Al-Si ordering in sodium feldspar (Salje et al. 1989) and potassium feldspar (Harris et al. 1989), and so it appears that such linear scaling (Salje 1992c) is generally obeyed in the feldspar structure. Following this argument further means that structural states in feldspars can be characterized equally well by

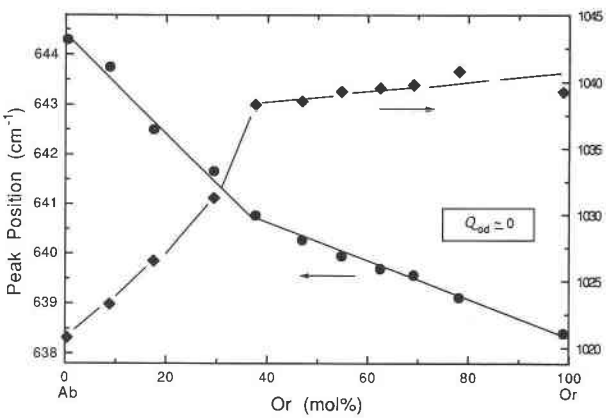


**FIGURE 15.** Compositional dependence of the phonon frequencies near 640 and 1030 $cm^{-1}$ ($Q_{od} = 0$).

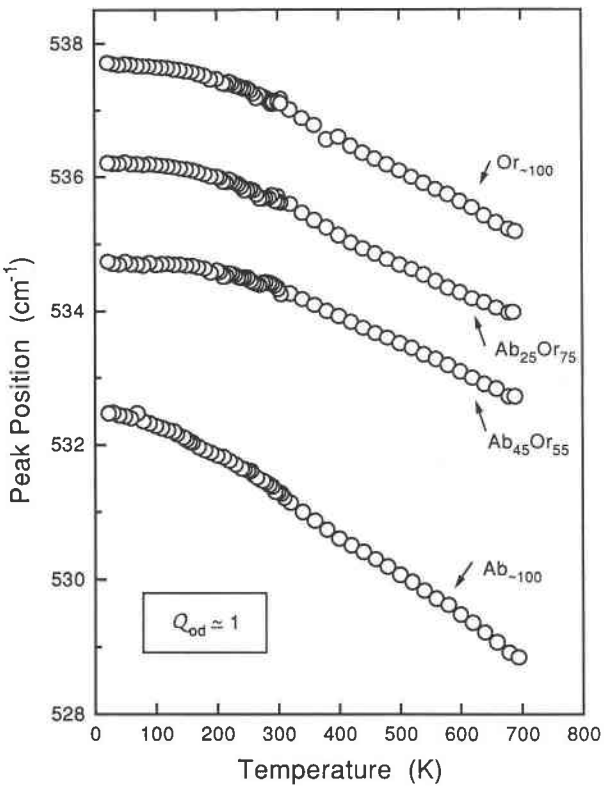


**FIGURE 16.** Temperature dependence of the phonon modes near 534 $cm^{-1}$ for $Ab_{100}$, $Ab_{45}Or_{55}$, $Ab_{25}Or_{75}$, and $Or_{100}$ ($Q_{od} \simeq 1$).

the width of phononic absorption profiles or the phonon frequency (i.e., the position of the phonon peak in the absorption spectrum).

A low-temperature anomaly in potassium feldspar occurs near 270 K. It manifests itself by subtle changes in the intensity and frequency of the 157 $cm^{-1}$ signal; no significant changes were found for other phonons (Fig. 4A). The temperature evolution of the intensity ratio $I_{146\,cm^{-1}}$/

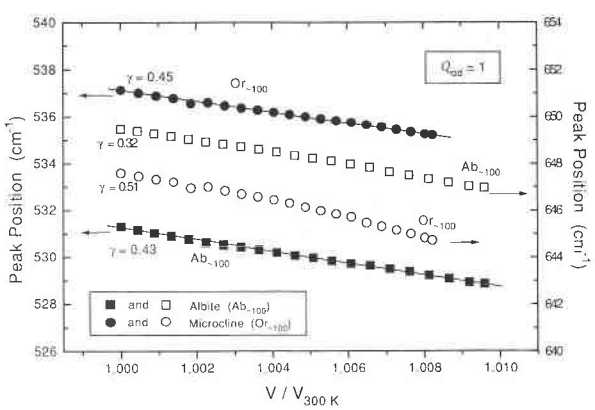


**FIGURE 17.** Linear volume dependence of two phonon frequencies for $Ab_{100}$ and $Or_{100}$ ($Q_{od} \simeq 1$). The slopes correspond to the mode Grüneisen parameters indicated in the graph [unit-cell volumes after Stewart and von Limbach (1967) and Openshaw et al. (1979)].

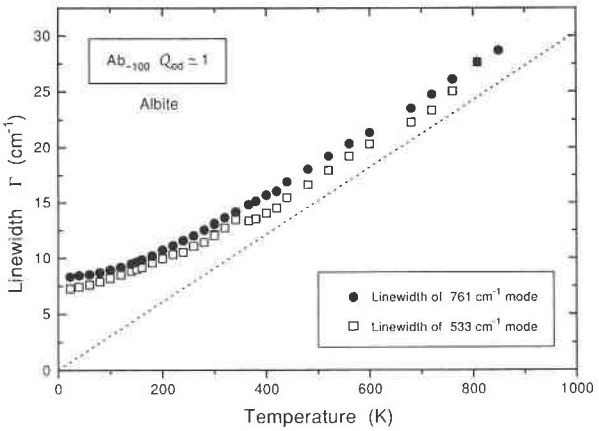


FIGURE 18. Temperature evolution of the line width of the absorption signals near 533 and 761 cm$^{-1}$ (Ab$_{100}$, $Q_{od} \simeq 1$).

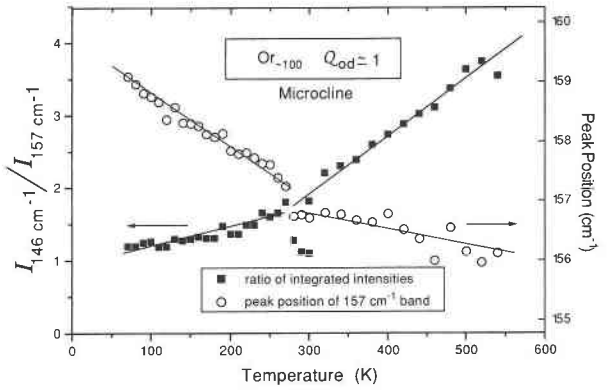


FIGURE 20. Temperature evolution of the ratio of the integral absorbances of the phonon signals at 146 and 157 cm$^{-1}$. A break in slope occurs near 270 K.

$I_{157\ cm^{-1}}$ and the frequency of the 157 cm$^{-1}$ mode appear to be linear below and above 270 K but show different slopes (Fig. 20). Although these changes are small, they are clearly larger than our experimental resolution. A somewhat similar observation was previously reported by Wyncke et al. (1981), although we did not observe other significant changes in the phonon spectra. We feel that more systematic structural work is necessary before we can identify this anomaly as an indication of structural phase transition in potassium feldspar.

### The effect of temperature on Na-O, K-O, and Si-O bond lengths

The temperature-induced frequency shifts of the low frequency phonon modes (Na-O stretching and K-O stretching modes) are usually taken as indicating an increase of the Na-O and K-O bond lengths with rising temperature. Such a correlation between frequency shifts and bond lengths is consistent with the results of previous X-ray diffraction studies, which show that most of the Na-O bond lengths for low albite increase with increasing temperature (Prewitt et al. 1976; Winter et al. 1979). The mean Na-O distance in high albite increased from 0.281 nm at 297 K to 0.286 nm at 1378 K (Prewitt et al. 1976). We now use a similar correlation for the discussion of the Si-O bond length, which has been rather controversial.

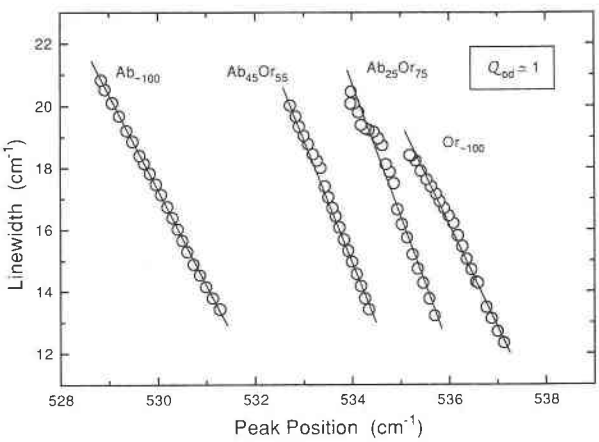


FIGURE 19. Correlation between the width of the absorption line and the phonon frequencies for the 532 cm$^{-1}$ mode in four alkali feldspars ($Q_{od} \simeq 1$).

The phonons associated with Si-O stretching in the region of 1000–1300 cm$^{-1}$ clearly exhibit frequency softening with increasing temperature between 20 and 850 K (Fig. 21). A typical shift is $\Delta\omega/\omega = 2.7\%$, with $\omega = 1202$ cm$^{-1}$ for this temperature range. The negative frequency shifts of the Si-O stretching modes indicate that the lengths of the Si-O bonds in $SiO_4$ tetrahedra increase with increasing temperature. The temperature effect on the Si-O distance and the crystal structure of feldspars is not fully understood, however. There have been a few published data on the variation of the crystal structure of alkali feldspars determined directly at high temperature (Prewitt et al. 1976; Winter et al. 1977, 1979; Downs et al. 1992). By comparing the crystal structure, Prewitt et al. (1976) found that the mean T-O distance decreased slightly with increasing temperature, whereas the mean Na-O distance increased in high albite. Winter et al. (1977) argued that the apparent contraction of T-O bonds with temperature in silicates probably resulted from errors in the analysis of the measured data caused by thermal motion and that some corrections were needed for the assessment of the bond distances. Their corrected T-O distance showed an increase with increasing temperature. Downs et al. (1992) also found, by analysis of the rigid motion of coordinated polyhedra, that the corrected bond length ($R_{TLS}$) almost always increases in a regular way with increasing temperature. Downs et al. (1992) and Armbruster et al. (1990) proposed, as one possible way to derive more realistic bond distances, to model the rigid-body motion of silicate tetrahedra in a manner consistent with the thermal motion data obtained from the refinement of X-ray diffraction intensities. For a detailed discussion of the variation of displacement parameters in

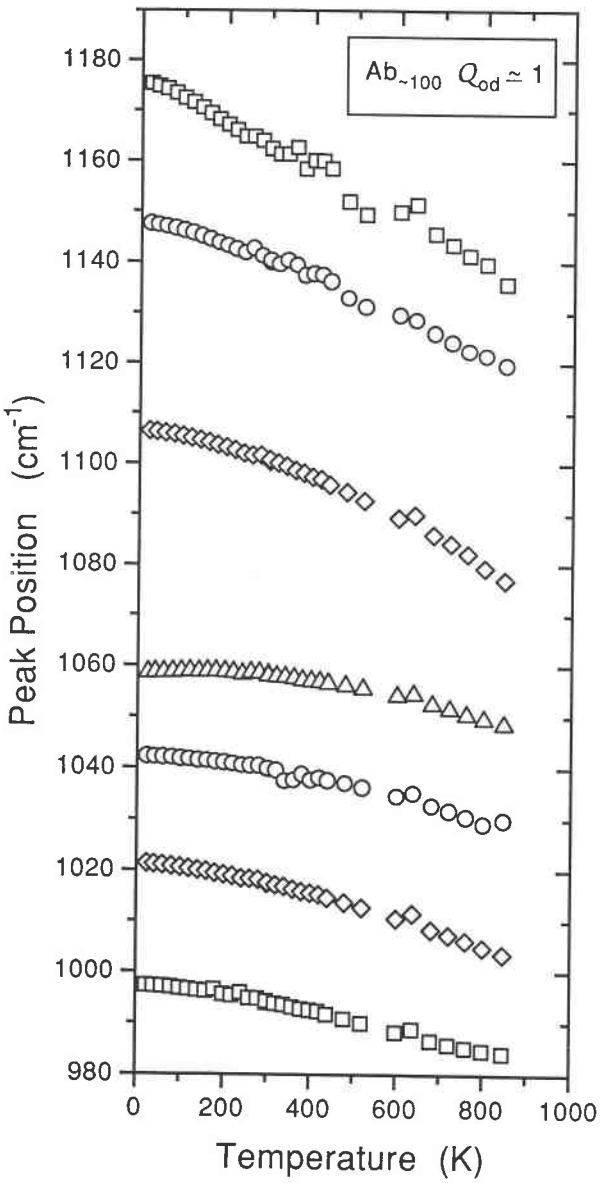


**FIGURE 21.** Temperature dependence of the positions of phonon absorption bands at high frequencies showing thermal softening of Si-O vibrations in sodium feldspar ($Ab_{100}$, $Q_{od} \simeq 1$).

the structure refinement of albite and the effect of Al-Si disorder in alkali feldspars, see Armbruster et al. (1990) and Kunz and Armbruster (1990). For the thermal effects, Downs et al. (1992) predicted that the $R_{TLS}$ would increase by 1.4% after heating from 15 to 1250 K. Our result that the Grüneisen parameters of the Si-O stretching modes are positive and, for tetrahedral complexes, unusually large, supports the idea of a substantial increase of the Si-O distance with increasing temperature.

## REFERENCES CITED

Armbruster, T., Bürgi, H.B., Kunz, M., Gnos, E., Brönnimann, S., and Lienert, C. (1990) Variation of displacement parameters in structure refinements of low albite. American Mineralogist, 75, 135–140.

Barron, T.H.K., Collins, J.F., Smith, T.W., and White, G.K. (1982) Thermal expansion, Grüneisen functions and static lattice properties of quartz. Journal of Physics C, 15, 4311–4326.

Bismayer, U. (1990) Hard mode Raman spectroscopy and its application to ferroelastic and ferroelectric phase transitions. Phase Transitions, 27, 211–267.

Bratkovsky, A.M., Marais, S.C., Heine, V., and Salje, E.K.H. (1994a) The theory of fluctuations and texture embryos in structural phase transitions mediated by strain. Journal of Physics: Condensed Matter, 6, 3679–3696.

Bratkovsky, A.M., Salje, E.K.H., and Heine, V. (1994b) Overview of the origin of tweed texture. Phase Transitions, 52, 77–83.

Bratkovsky, A.M., Salje, E.K.H., Marais, S.C., and Heine, V. (1994c) Theory and computer simulation of tweed texture. Phase Transitions, 48, 1–13.

Brown, W.L., and Parsons, I. (1994) Feldspars in igneous rocks. In I. Parsons, Ed., Feldspars and their reactions, p. 449–499. Kluwer, Dordrecht, the Netherlands.

Downs, R.T., Gibbs, G.V., Bartelmehs, K.L., and Boisen, M.B. (1992) Variations of bond lengths and volumes of silicate tetrahedra with temperature. American Mineralogist, 77, 751–757.

Grundy, H.D., Brown, W.L., and MacKenzie, W.S. (1967) On the existence of monoclinic $NaAlSi_3O_8$ at elevated temperatures. Mineralogical Magazine, 36, 83–88.

Harris, M.J., Salje, E., Güttler, B.K., and Carpenter, M.A. (1989) Structural states of natural potassium feldspar: An infrared spectroscopic study. Physics and Chemistry of Minerals, 16, 649–658.

Harrison, R.J., and Salje, E.K.H (1994) X-ray diffraction study of the displacive phase transition in anorthoclase, grain-size effects and surface relaxations. Physics and Chemistry of Minerals, 21, 325–329.

Haselton, H.T., Jr., Hovis, G.L., Hemingway, B.S., and Robie, R.A. (1983) Calorimetric investigation of the excess entropy of mixing in analbite-sanidine solid solutions: Lack of evidence for Na,K short-range order and implications for two-feldspar thermometry. American Mineralogist, 68, 398–413.

Henderson, C.M.B. (1979) An elevated temperature X-ray study of synthetic disordered Na-K alkali feldspars. Contributions to Mineralogy and Petrology, 70, 71–79.

Hofmeister, A.M., and Rossman, G.R. (1984) Determination of $Fe^{3+}$ and $Fe^{2+}$ concentrations in feldspar by optical absorption and EPR Spectroscopy. Physics and Chemistry of Minerals, 11, 213–224.

Iiishi, K., Tomisaka, T., Kato, T., and Umegaki, Y. (1971a) Isomorphous substitution and infrared and far infrared spectra of the feldspar group. Neues Jahrbuch für Mineralogie Abhandlungen, 115, 98–119.

——— (1971b) The force field of K feldspar. Zeitschrift für Kristallographie, 134, 213–229.

Kroll, H., Bambauer, H.-U., and Schirmer, U. (1980) The high albite-monalbite and analbite-monalbite transitions. American Mineralogist, 65, 1192–1211.

Kroll, H., Schmiemann, I., and von Cölln, G. (1986) Feldspar solid solutions. American Mineralogist, 71, 1–16.

Kunz, M., and Armbruster, T. (1990) Difference displacement parameters in alkali feldspars: Effects of (Si,Al) order-disorder. American Mineralogist, 75, 141–149.

Laves, F., and Hafner, S. (1956) Ordnung/Unordnung und ultrarotabsorption: I. (Al,Si)-Verteilung in Feldspäten. Zeitschrift für Kristallographie, 108, 52–63.

Mackenzie, W.S. (1952) The effect of temperature on the symmetry of high-temperature soda-rich feldspars. American Journal of Science, Bowen volume, 250A, 319–342.

Okamura, F.O., and Ghose, S. (1975) Analbite → monalbite transition in a heat treated twinned Amelia albite. Contributions to Mineralogy and Petrology, 50, 211–216.

Openshaw, R.E., Henderson, C.M.B., and Brown, W.L. (1979) A room-temperature phase transition in maximum microcline: Unit cell parameters and thermal expansion. Physics and Chemistry of Minerals, 5, 95–104.

Petrov, I., Mineeva, R.M., Bershov, L.V., and Agel, A. (1993) EPR of $[Pb\text{-}Pb]^{3+}$ mixed valence pairs in amazonite-type microcline. American Mineralogist, 78, 500–510.

Phillips, B.L., Kirkpatrick, R.J., and Hovis, G.L. (1988) $^{27}Al$, $^{29}Si$ and

$^{23}$Na MAS NMR study of an Al,Si ordered alkali feldspar solid solution series. Physics and Chemistry of Minerals, 16, 262–275.

Prewitt, C.T., Sueno, S., and Papike, J.J. (1976) The crystal structures of high albite and monalbite at high temperatures. American Mineralogist, 61, 1213–1225.

Putnis, A., and Salje, E.K.H. (1994) Tweed microstructures: Experimental observations and some theoretical models. Phase Transitions, 48, 85–105.

Salje, E.K.H. (1985) Thermodynamics of sodium feldspar: I. Order parameter treatment and strain induced coupling effects. Physics and Chemistry of Minerals, 12, 93–98.

——— (1986) Raman spectroscopic investigation of the order parameter behaviour in hypersolvus alkali feldspar: Displacive phase transition and evidence for Na-K site ordering. Physics and Chemistry of Minerals, 13, 340–346.

——— (1990) Phase transitions in ferroelastic and co-elastic crystals, 366 p. Cambridge University Press, Cambridge.

——— (1991) Crystallography and structural phase transitions, an introduction. Acta Crystallographica, A47, 453–469.

——— (1992a) Application of Landau theory for the analysis of phase transitions in minerals. Physics Reports, 215(2), 49–99.

——— (1992b) Phase transitions in minerals: From equilibrium properties towards kinetic behavior. Berichte der Bunsen-Gesellschaft für physikalische Chemie, 96(11), 1518–1541.

——— (1992c) Hard mode spectroscopy: Experimental studies of structural phase transitions. Phase Transitions, 37, 83–110.

——— (1993) On the kinetics of partially conserved order parameters: A possible mechanism for pattern formation. Journal of Physics: Condensed Matter, 5, 4775–4784.

——— (1994) Phase transitions and vibrational spectroscopy in feldspars. In I. Parsons, Ed., Feldspars and their reactions, p. 103–160. Kluwer, Dordrecht, the Netherlands.

Salje, E.K.H., Kuscholke, B., Wruck, B., and Kroll, H. (1985) Thermodynamics of sodium feldspar: II. Experimental results and numerical solutions. Physics and Chemistry of Minerals, 12, 99–107.

Salje, E.K.H., Güttler, B., and Ormerod, C. (1989) Determination of the degree of Al,Si order $Q_{od}$ in kinetically disordered albite using hard mode infrared spectroscopy. Physics and Chemistry of Minerals, 16, 576–581.

Salje, E.K.H., and Kroll, H. (1991) Kinetic rate laws derived from order parameter: III. Al,Si ordering in sanidine. Physics and Chemistry of Minerals, 17, 563–568.

Salje, E.K.H., Wruck, B., and Marais, S. (1991a) Order parameter saturation at low temperatures: Numerical results for displacive and O/D systems. Ferroelectrics, 124, 185–188.

Salje, E.K.H., Wruck, B., and Thomas, H. (1991b) Order-parameter saturation and a low-temperature extension of Landau theory. Zeitschrift für Physik B, 82, 399–404.

Salje, E.K.H., Bismayer, U., Wruck, B., and Hensler, J. (1991c) Influence of lattice imperfections on the transition temperatures of structural phase transitions: The plateau effect. Phase Transitions, 35, 61–74.

Salje, E.K.H., Wruck, B., Graeme-Barber, A., and Carpenter, M.A. (1993) Experimental test of rate equations: Time evolution of Al,Si ordering in anorthite $CaAl_2Si_2O_8$. Journal of Physics: Condensed Matter, 5, 2961–2968.

Smith, J.V., and Brown, W.L. (1988) Feldspar minerals, vol. 1, 828 p. Springer, Heidelberg, Germany.

Stewart, D.B., and von Limbach, D. (1967) Thermal expansion of low and high albite. American Mineralogist, 52, 389–413.

Tsatskis, I., Salje, E.K.H., and Heine, V. (1994) Pattern formation during phase transitions: Kinetics of partially conserved order parameters and the role of gradient energies. Journal of Physics: Condensed Matter, 6, 11027–11034.

von Stengel, M.O. (1977) Normalschwingungen von Alkalifeldspäten. Zeitschrift für Kristallographie, 146, 1–18.

Winter, J.K., Ghose, S., and Okamura, F.P. (1977) A high-temperature study of the thermal expansion and the anisotropy of the sodium atom in low albite. American Mineralogist, 62, 921–931.

Winter, J.K., Okamura, F.P., and Ghose, S. (1979) A high-temperature structural study of high albite, monalbite, and the analbite → monalbite phase transition. American Mineralogist, 64, 409–423.

Wruck, B., Salje, E.K.H., and Graeme-Barber, A. (1991) Kinetic rate laws derived from order parameter theory: IV. Kinetics of Al-Si disordering in Na-feldspars. Physics and Chemistry of Minerals, 17, 700–710.

Wyncke, B., McMillan, P.F., Brown, W.L., Openshaw, R.E., and Bréhat, F. (1981) A room-temperature phase transition in maximum microcline: Absorption in the far infrared (10–200 $cm^{-1}$) in the temperature range 110–300 K. Physics and Chemistry of Minerals, 7, 31–34.

Manuscript received January 20, 1995
Manuscript accepted August 25, 1995